Photoluminescence Excitation Spectroscopy for In-Line Optical Characterization of Crystalline Solar Cells

Dionisis Berdebes, *Student Member, IEEE*, Jayprakash Bhosale, Kyle H. Montgomery, *Member, IEEE*, Xufeng Wang, *Student Member, IEEE*, Anant K. Ramdas, Jerry M. Woodall, *Fellow, IEEE*, and Mark S. Lundstrom, *Fellow, IEEE*

***Abstract*—Techniques to permit in-line characterization during various stages of solar cell research, development, and manufacturing provide a convenient means for optimizing yield, cost, and efficiency. Photoluminescence measurements are widely used for material characterization. This paper examines photoluminescence excitation spectroscopy (PLE) in which the steady-state photoluminescence is monitored as a function of the wavelength of the incident illumination. The use of PLE for in-line optical characterization of direct bandgap crystalline solar cells is explored. With a novel LED-based setup, we measure the PLE response of a GaAs solar cell. Using drift-diffusion numerical simulations, we evaluate the relation between PLE and EQE measurements, and also compare the PLE measurement with the corresponding EQE measurement in order to establish the correspondence between the two techniques.**

***Index Terms*—Crystalline materials, photoluminescence, photovoltaic cells.**

I. Introduction

THE continuous search for efficient, reliable, and inexpensive solar cell materials and structures demands a characterization technique with quick feedback for optimizing solar cell fabrication processes. Hence, in-line monitoring techniques that do not require the fabrication of completed solar cells can play an important role in solar cell research, development, and manufacturing. Photoluminescence (PL) measurements, especially in the form of time-resolved PL decay are widely used [1]. The various types of photoluminescence excitation spectroscopy (PLE) are also widely used for material characterization [2]–[4]. In this paper, we examine a technique that has been used to study GaAs solar cells and that can, under the right conditions, predict the external quantum efficiency (EQE) of a complete solar cell for a contacted structure.

To conduct a PLE measurement, a monochromatic light flux $\phi_{\rm exc}(\lambda_{\rm exc})$ photogenerates free carriers in the solar cell device under open-circuit conditions. Some of the free carriers subsequently recombine radiatively and emit a PL signal, $\phi_{\rm emit}$, that is collected, while the rest recombines nonradiatively. The PLE efficiency is defined as

$$\mathrm{PLE}(\lambda_{\rm exc}) = \phi_{\rm emit}/\phi_{\rm exc}(\lambda_{\rm exc}). \tag{1}$$

Exploiting the fact that the radiative recombination can be spatially dependent, the PLE measurements are useful in deriving surface and bulk recombination parameters [5], [6].

Another common solar cell characterization technique is the measurement of the external quantum efficiency. In an EQE measurement, free carriers are photogenerated with an excitation spectrum as in PLE, and for each excitation wavelength, the short circuit current, $J_{\rm sc}$, is measured. The EQE is defined as

$$\mathrm{EQE}(\lambda_{\rm exc}) = J_{\rm sc}/q\phi_{\rm exc}(\lambda_{\rm exc}). \tag{2}$$

The EQE measurement is a standard, widely deployed technique in solar cell characterization that can provide information such as optical losses, surface and bulk recombination, and material bandgap. A drawback of the EQE measurement is the requirement for electrical contacts, which is typically one of the very last steps in the cell fabrication process, thus, rendering it unfit for in-line characterization, which the PLE measurement, on the other hand, is perfectly suited for.

Pettit *et al*. [5] and Woodall *et al*. [6] have shown experimentally for a GaAs solar cell, that the PLE and EQE measurements have similar spectral shape. Subsequent work by Rau [7], [8] showed analytically that there is a fundamental connection between EQE and electroluminescent emission, and this relation has been used by Green [9] to indirectly deduce the external radiative efficiency of a cell from its measured EQE. If a clear connection can be established between the EQE and PLE spectra, then the usefulness of the EQE measurement can be extended into the in-line characterization where it is much needed.

Manuscript received June 17, 2013; revised July 27, 2013; accepted August 6, 2013. Date of publication September 4, 2013; date of current version September 18, 2013. This work was supported by the Semiconductor Research Corporations Energy Research Initiative (ERI) through the Network for Photovoltaic Technology (NPT). The Computational support was provided by the Network for Computational Nanotechnology (NCN). The work of K. H. Montgomery was supported by the Air Force Research Laboratory for providing the GaAs sample. The work of A. K. Ramdas was supported by the National Science Foundation under Grant DMR 0705793. D. Berdebes, J. Bhosale, and K. H. Montgomery contributed equally to this work.

D. Berdebes, X. Wang, and M. S. Lundstrom are with the Network for Photovoltaic Technology, School of Electrical and Computer Engineering, Purdue University, West Lafayette, IN 47906 USA (e-mail: dionisis@purdue.edu; wang159@purdue.edu; lundstro@purdue.edu).

J. Bhosale and A. K. Ramdas are with the Department of Physics, Purdue University, IN 47907 USA (e-mail: jbhosale@purdue.edu; akr@purdue.edu).

K. H. Montgomery and J. M. Woodall are with the Department of Electrical and Computer Engineering, University of California, CA 95616 USA (e-mail: kmontgomery@ucdavis.edu; jwoodall@ucdavis.edu).

Color versions of one or more of the figures in this paper are available online at http://ieeexplore.ieee.org.

Digital Object Identifier 10.1109/JPHOTOV.2013.2278884

In this paper, we explore the relationship between PLE and EQE spectra, describe a simple LED-based instrumentation for PLE studies, and illustrate this technique by measurement on a GaAs solar cell. In Section II, we use detailed numerical simulations of a model GaAs p-n junction solar cell to compare the EQE and PLE spectra. We study the sensitivities of the two spectra to transport properties and to bulk/interfacial recombination, and establish the conditions for which the two spectra are similar. Section III describes the LED-based instrumentation, and the corresponding PLE and EQE measurements on a GaAs solar cell. In Section IV, we comment on the criteria for a spectral similarity between the PLE and EQE. Finally, we conclude and summarize the findings in Section V.

II. Numerical Studies

A. Simulation Method

To examine the connection between PLE and EQE measurements, the numerical simulations of model structures were conducted. The numerical simulator solves the continuity equations for electrons and holes, coupled with Poisson's equation, using a simple Beer's law treatment of optical absorption. For these studies, we used the ADEPT simulation program [10].

From the simulation for a specific wavelength of illumination, $\lambda_{\rm exc}$, the position dependent radiative recombination rate, $R_{\rm rad} = B(n(x)p(x) - n_i^2)$, is obtained (here $n(x)$ and $p(x)$ represent the nonequilibrium carrier densities for electrons and holes, respectively, and n_i is the intrinsic carrier density). The radiative recombination profile is then numerically integrated across the device to obtain the total radiative recombination within the device. The photoluminescence signal $I_{\rm PL} = f(\lambda_{\rm exc})$ is assumed to be proportional to the total radiative recombination within the device. Note that this approach does not account for self-absorption and photon recycling effects. A fully self-consistent electrical/optical model that treats these effects [11] was used to test a few specific cases, and no significant differences were found, if an effective value of $B = 3 \times 10^{-10}{\rm cm}^3/{\rm s}$ was used.

B. Device Simulation

A high quality GaAs p-n junction, whose band diagram is shown in Fig. 1(a), is considered first. The mobilities of electrons and holes in the n-type absorber are set at $\mu_e = 3000\ {\rm cm}^2/{\rm V}\cdot{\rm s}$ and $\mu_h = 150\ {\rm cm}^2/{\rm V}\cdot{\rm s}$, respectively, while for the p-type emitter $\mu_e = 4000\ {\rm cm}^2/{\rm V}\cdot{\rm s}$ and $\mu_h = 250\ {\rm cm}^2/{\rm V}\cdot{\rm s}$. The absorption spectrum is obtained from the experimental data in [12], and front and back surface recombination is assumed to be zero. A radiative recombination coefficient of $B = 3 \times 10^{-10}\ {\rm cm}^3/s$ was assumed, yielding a radiative lifetime of $\tau_{\rm rad} = 30$ ns, which is considerably shorter than the nonradiative $\tau_{\rm SRH} = 100\ \mu$s. With the aforementioned parameters, a diffusion length of $L_p \simeq 3.4\ \mu$m is deduced, which is larger than the absorber thickness, and explains the high EQE values and the good carrier collection as observed in Fig. 1(b). Fig. 1(b) also shows the simulated PLE spectrum under open-circuit conditions with monochromatic excitation in the range of 400–900 nm.

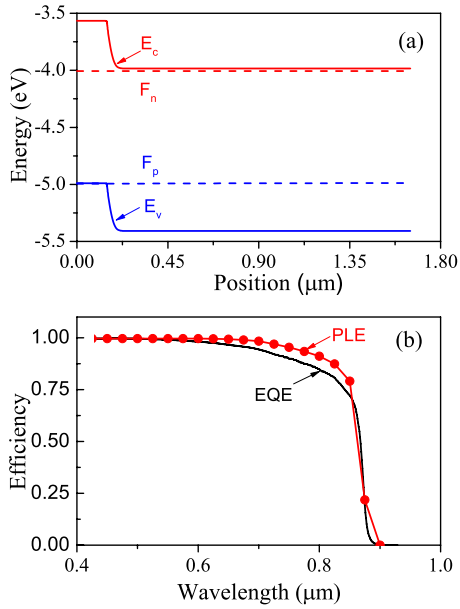

Fig. 1. (a) Band diagram of the model p-n junction device under open-circuit conditions and monochromatic excitation at $\lambda = 500$nm. (b) Simulated EQE and PLE spectra of the model p-n junction device, with the PLE spectra simulated under open-circuit conditions.

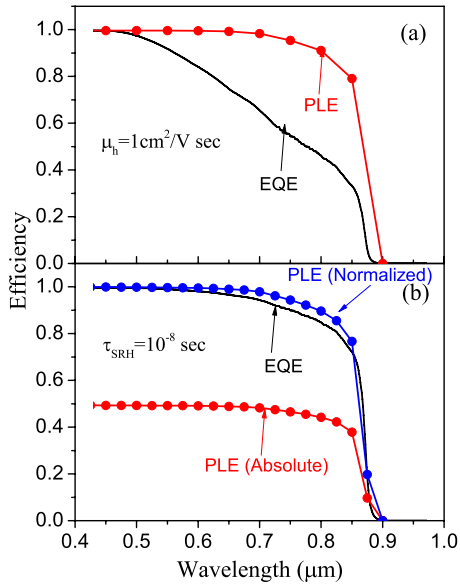

Fig. 2. Simulated PLE and EQE spectra of p-n junction device, with (a) $\mu_h = 1\ {\rm cm}^2/{\rm V}\cdot{\rm s}$ and (b) $\tau_{\rm SRH} = 10$ ns.

As Fig. 1(b) shows the open-circuited PLE and the short-circuited EQE spectra are essentially identical for this model structure.

In order to examine the similarity between EQE and PLE, we simulate these spectra under three different conditions associated with transport and surface/bulk recombination.

1) Mobility: Real solar cell mobilities are often considerably smaller than those assumed for the model device, especially for thin film materials. Fig. 2(a) shows the comparison between PLE and EQE for an absorber with hole mobility $\mu_h = 1\ {\rm cm}^2/{\rm V}\cdot{\rm s}$, which corresponds to a diffusion length of $L_p = 0.28\ \mu$m. The

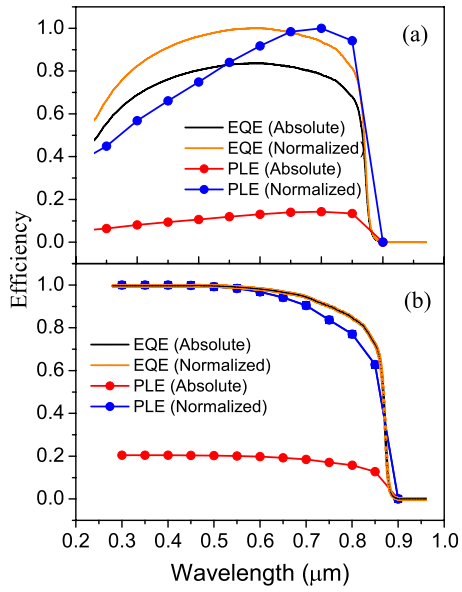

Fig. 3. Simulated PLE and EQE spectra of p-n junction device, with surface recombination velocity set to $s_f/(s_b) = 10^7$ cm/s at (a) front surface, and (b) back surface. For the latter case, only the absolute EQE is shown, since the normalized and the absolute EQE coincide.

main features observed are: 1) the suppression of EQE at longer wavelengths due to poorer carrier collection, and 2) the insensitivity of the PLE response to mobility degradation. The difference is readily understood. The low carrier mobility reduces the diffusion length, which lowers carrier collection and the EQE, but the low mobility does not affect the internal quantum efficiency; therefore, the PLE spectrum is unchanged.

2) Lifetime: Nonradiative recombination can significantly influence both the PL intensity, and the collected photocurrent. In order to explore the effect of lifetime, we reduced an SRH lifetime to $\tau_{\rm SRH} = 10$ ns. Fig. 2(b) shows the PLE and EQE spectra simulated for this case. The EQE response is unaffected, because the minority carrier diffusion length $L_p \simeq 1.7$ μm is still long enough for good carrier collection. In this case, the nonradiative lifetime $\tau_{\rm nr} = 10$ ns becomes comparable to the radiative lifetime $\tau_r = 30$ ns. We see a significant drop in absolute magnitude for the PLE, but no significant difference in the qualitative shape between the PLE and EQE spectra can be observed.

3) Surface Recombination: Finally, we examine the effect of surface recombination on PLE and EQE spectra. First, the front surface recombination velocity was set at $s_f = 10^7$ cm/s, and the back at $s_b = 0$ cm/s. The effect on the PLE spectrum is shown in Fig. 3(a). A large front surface recombination velocity leads to an overall degradation of the PLE signal as well as to a strong suppression for short wavelengths, when the generation occurs primarily close to the front surface recombination sink. The short wavelength EQE also shows a similar trend. Next, the same surface recombination velocity of $s_b = 10^7$ cm/s was chosen for the rear surface, and the front surface was set to $s_f = 0$ cm/s. In this case, as seen in Fig. 3(b), the PLE and EQE spectra display a similar degradation of overall intensity, but the intensity suppression now occurs at longer wavelengths.

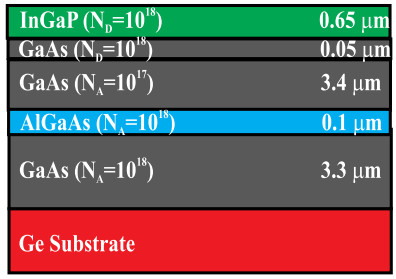

Fig. 4. Structure of the GaAs solar cell.

A discussion of the aforementioned simulation findings with the use of an analytical model is provided in Section IV. To summarize, simulation of model structures show that the short-circuit EQE, and open-circuit PLE spectra display similar shapes, and, under the right conditions, can even be identical.

III. Experimental Studies

To demonstrate that PLE works as the simulations discussed in Section II suggest that experimental studies were conducted on a high-quality GaAs solar cell. Considering the application of this study as an in-line contact-less technique for solar cell characterization, a novel cost-effective instrumentation, based on LED sources was developed. This approach coupled with the simulation techniques provides a reliable characterization of solar cell devices in industrial and research applications.

A. Sample Preparation

Measurements were carried out on a GaAs solar cell whose structure is shown in Fig. 4. The cell was designed as an isotype cell from a triple junction solar cell one. Starting from the top, the structure consists of a n-type GaAs top contact layer, followed by an InGaP ($E_g = 1.87$ eV) window layer, which transmits light for $\lambda_{\rm exc} > 600$ nm. The active homojunction consists of a n-type emitter with a thickness $w = 0.05$ μm, and doping density $N_D \simeq 10^{18}$/cm^3 on the top of a GaAs p-type absorber with doping density $N_A \simeq 10^{17}$/cm^3, and a thickness $w = 3.4$ μm. At the bottom of the absorber is a 0.1 μm AlGaAs back surface field layer, a 3.3 μm GaAs buffer layer, and the Ge substrate. All layers were epitaxially grown by organometallic vapor phase epitaxy (OMVPE).

B. Instrumentation

A PLE measurement requires an equal number of optical carrier generation at different excitation wavelengths, which means a constant photon flux at each excitation wavelength. Hence, the incident radiation power must be inversely proportional to the excitation wavelength. In addition, a sufficient temporal stability of the incident photon flux is desired for a reliable PLE acquisition. As a source for optical spectroscopy, LEDs possess all the desired features which the incandescent and arc lamps lack. With the anticipated increase in brightness and luminous efficiency [13] (particularly at shorter wavelengths) along with their small size and low cost, LEDs offer significant improvement over conventional sources for PLE spectroscopy. With

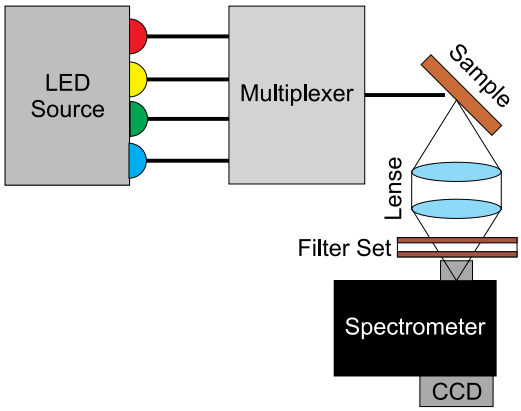

Fig. 5. PLE setup with LED source for the monochromatic illumination of a sample.

additional current and temperature tuning of suitable LEDs, higher intensity can be extended to desired wavelengths in order to obtain improved resolution in the PLE spectra. The PLE setup shown in Fig. 5 consists of a temperature controlled LED source [14] containing a set of bright LEDs optically coupled to a multiplexer which selects the radiation from a desired LED. The output radiation from the multiplexer is then illuminated on the cell with an optical fiber. The PL radiation generated by the sample is then collected and focused on the entrance slit of a spectrometer for spectral analysis. In contrast with an EQE measurement, a PLE measurement requires additional instrumentation to reliably detect low PL intensity with the background of scattered excitation light. The LEDs used in this study easily provide up to 10 mW/mm^2 of incident radiation density in order to generate a PL signal with sufficient S/N under a typical low-level injection condition. Furthermore, lock-in detection was used to improve the detection sensitivity for samples exhibiting extremely weak PL. In this case, the rapid switching capability of the LEDs was exploited to eliminate the need for a mechanical chopper typically used in this technique. The excitation light scattered from the sample along the optical path of the spectrometer was eliminated with a set of high optical density bandpass filters placed in front of the spectrometer. In order to avoid the spectral region overlap of the scattered radiation and that of the filter passband, appropriate LEDs were used with temperature tuning.

C. Experimental Results

Fig. 6(a) shows the measured PL spectrum of the GaAs solar cell with 720 nm LED excitation. A constant photon flux of 9×10^{15} photons/s was maintained for all the excitation wavelengths. The spectral width of the LEDs varied from 20 nm FWHM at 440 nm, to 30 nm FWHM at 780 nm. Simulations indicate that the spectral width of the LED does not have a significant effect on the measured PL spectrum. Measurements with excitation wavelengths near the absorption edge are difficult due to the overlap of the spectral region between LED radiation and PL emission. Fig. 6(b) shows a comparison of the experimentally observed PLE and EQE spectra. The PLE data

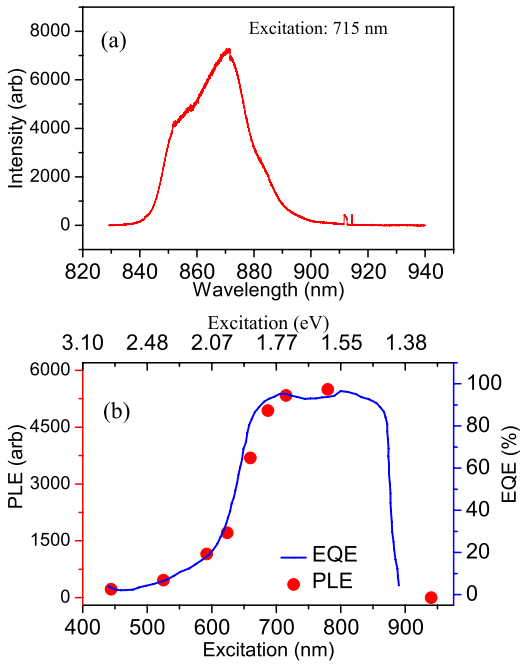

Fig. 6. (a) PL spectrum of the solar cell at the 720 nm excitation. (b) Comparison of measured EQE and PLE spectra for GaAs homo-junction solar cell. The PLE spectra was measured with a constant photon flux of 9×10^{15} photons/s.

points represent the intensity of the emitted PL signal at 870 nm [the peak of the emission in Fig. 6(a)]. In a typical PL experiment, only a fraction of the emitted photons are collected, so the PLE spectrum is scaled in order to match the magnitude of EQE spectrum. The constant background in the PL spectrum due to the combination of detector offset and stray light is subtracted from the intensity measurements in order to match the zero of the EQE spectrum. The comparison indicates that the result is in good agreement with the simulations for a high-quality junction. The sharp drop near 700 nm in both EQE and PLE is due to the absorption of InGaP window layer, which inhibits light flux from reaching the GaAs layer, and consequently affects both spectra.

IV. Discussion

As discussed in Section II, the short-circuit EQE, and open-circuit PLE are not always equivalent. For example, in case of a perfect absorbing solar cell with long and equal nonradiative $(\tau_{\rm nr})$, and radiative (τ_r) lifetimes, the PLE signal has a magnitude of 50%, but the EQE signal approaches 100%, since recombination under short-circuit conditions is minimal, but the internal quantum efficiency (relevant for PLE under open-circuit conditions) is 50%. As discussed in Section II, however, there are similarities between the EQE and PLE spectra, and the differences can, in principle, be used to deduce more information than could be obtained from an EQE or PLE measurement alone. To better understand the connection between the EQE and PLE, we start with their definitions (1), and (2).

In terms of the absorbance $a(\lambda_{\rm exc}) = G_{\rm TOT}(\lambda_{\rm exc})/\phi_{\rm exc}(\lambda_{\rm exc})$, where $G_{\rm TOT}(\lambda_{\rm exc})$ is the total generation in the

cell, the definition of EQE becomes

$$\begin{aligned}\mathrm{EQE}(\lambda_{\mathrm{exc}}) &= a(\lambda_{\mathrm{exc}}) \times \frac{J_{\mathrm{sc}}/q}{G_{\mathrm{TOT}}(\lambda_{\mathrm{exc}})} \\ &= a(\lambda_{\mathrm{exc}}) \times \eta_{\mathrm{TOT}}^{\mathrm{coll}}. \end{aligned} \quad (3)$$

where $\eta_{\mathrm{TOT}}^{\mathrm{coll}}$ is the internal collection efficiency, the fraction of the photogenerated carriers that are collected by the junction.

The PLE is evaluated under open-circuit conditions for which the sum of the radiative ($R_{\mathrm{rad}}^{\mathrm{TOT}}$), and nonradiative recombination ($R_{\mathrm{nr}}^{\mathrm{TOT}}$) equals to the total generation rate $G_{\mathrm{TOT}}(\lambda_{\mathrm{exc}})$. The PLE definition (1) becomes

$$\begin{aligned}\mathrm{PLE}(\lambda_{\mathrm{exc}}) &= a(\lambda_{\mathrm{exc}}) \times (R_{\mathrm{rad}}^{\mathrm{TOT}}/(R_{\mathrm{rad}}^{\mathrm{TOT}} + R_{\mathrm{nr}}^{\mathrm{TOT}})). \\ &= a(\lambda_{\mathrm{exc}}) \times \gamma_{\mathrm{int}}. \end{aligned} \quad (4)$$

where γ_{int} is the internal quantum efficiency, the fraction of recombination events that are due to radiative recombination.

Based on equations (3) and (4), the criteria for spectral similarity between EQE and PLE can be identified. First, the EQE depends on the specific value of the lifetime (both radiative and nonradiative), because the lifetime determines the diffusion length, which controls the internal collection efficiency $\eta_{\mathrm{TOT}}^{\mathrm{coll}}$, while the PLE signal depends only on the ratio of the nonradiative to radiative lifetimes $\tau_{\mathrm{nr}}/\tau_r$. In addition, both EQE and PLE are approximately equal to the absorbance $a(\lambda_{\mathrm{exc}})$, when recombination losses are minimal ($\eta_{\mathrm{TOT}}^{\mathrm{coll}} \simeq 1$), and the internal quantum efficiency high ($\gamma_{\mathrm{int}} \simeq 1$). In this context, we now examine, how the results in Sections II and III can be explained with the use of (3) and (4).

1) Mobility: For the case of low mobility, the PLE response is not modified, since the absorbance $a(\lambda_{\mathrm{exc}})$, and the internal quantum efficiency in (4) are unchanged. For EQE, the mobility reduction decreases the diffusion length to $L_n = 0.11$ μm. In Fig. 2(a), one diffusion length L_n away from the depletion edge corresponds to 330 nm from the front surface. For most carriers to be absorbed within that region, an absorption coefficient value higher than $\sim 3 \times 10^4$/cm is required. This value corresponds to the typical absorption coefficient of p-type GaAs at ~600 nm, which explains the significant EQE drop starting at ~600 nm that we observed in Fig. 2(b).

2) Lifetime: By reducing the nonradiative lifetime from $\tau_{\mathrm{nr}} = 100$ μs to $\tau_{\mathrm{nr}} = 10$ ns, the internal quantum efficiency decreases from 99.7% to 22.5%, leading to a significant suppression of the PLE signal. The total lifetime $1/\tau_{\mathrm{eff}} = 1/\tau_r + 1/\tau_{\mathrm{nr}}$ decreases from $\tau_{\mathrm{eff}} = 30$ ns to $\tau_{\mathrm{eff}} = 7.5$ ns, which reduces the diffusion length from $L_p = 3.4$ μm to $L_p = 1.7$ μm. The diffusion length is relatively long in both cases, and, therefore, no significant change is observed in the EQE [see Fig. 2(a)].

3) Surface Recombination: In our numerical simulation, surface recombination is modeled as a boundary condition for diffused carriers that recombine at a surface sink. For a doping density of $N_D \simeq 10^{18}$/cm^3, the effect of surface band bending due to trap states is expected to be negligible [15], and, therefore, the surface recombination velocity numerical model should be sufficient. Correspondingly, in the analytical model, surface recombination is equivalent to recombination of electron-hole pairs close to the front surface that are not swept through the junction, and, therefore, effectively reduce the γ_{int}. In the case of a bad front surface, we observed significant decrease of the PLE and EQE in the short wavelength region, with the suppression in the PLE case being more pronounced, since, under open-circuit conditions, carriers are not collected, and, therefore, recombine more effectively at the front surface. In the case of a bad rear surface, the effect on $a(\lambda_{\mathrm{exc}})$ is minimal since the majority of the incoming light has been absorbed before reaching the back. Therefore, only the PLE suffered an overall decrease in magnitude due to the lowered γ_{int}.

So far, we have analyzed the connection between the PLE and EQE, and described the conditions for their spectral similarity. In experiments such as our LED-based setup in Section III and in previous studies [5] and [6], the normalized PLE and EQE from a GaAs solar cell are similar. We attribute this general agreement to the dominance of the absorbance term $a(\lambda_{\mathrm{exc}})$ in (3) and (4). In the simulation section of our study, the normalized PLE and EQE showed similar spectral shape in all scenarios except the one with low mobility. GaAs and other crystalline materials have mobility that is typically too high to observe any significant drop in the J_{sc}. Therefore, it is plausible to conclude that, in the case of high quality crystalline solar cells, the spectral dependence of both EQE and PLE largely depends on the absorbance factor $a(\lambda_{\mathrm{exc}})$.

The absolute magnitude of the PLE efficiency can also provide useful information about the recombination processes in the sample, since the radiative recombination intensity measurement $\int_0^w R_{\mathrm{Rad}}\, dx = \int_0^w R_{\mathrm{Rad0}} * (e^{(q\Delta E_f(x)/k_B T)} - 1)\, dx$ is effectively a quasi-Fermi level ΔE_f separation measurement. In this sense, it performs as a contactless voltage probe. As observed in Figs. 2(b), 3(a), and 3(b), PL efficiency can be strongly affected by factors such as surface and bulk recombination. In our experimental setup, we were unable to monitor absolute photon flux and, therefore, we did not investigate this specific aspect. In the case of a relative calibration of two solar cells with equal EQE efficiencies, the observed differences in the PLE efficiency should be directly related to changes in V_{oc}, and, therefore, can be used as an important, industrial solar cell quality test metric [16].

V. Conclusion

The results of this study provide additional support to the conclusion of previous work [5], [6] that PLE is a useful in-line characterization approach for solar cells. Our experimental studies, based on a novel LED-based setup, showed that in the case of a high-quality GaAs solar cell, where the absorption losses become dominant over recombination losses, the two measurements show remarkable agreement. Drift-diffusion simulations on a model GaAs solar cell junction, corroborate well with the experimental observation. Simulation scenarios of suppressed nonradiative recombination lifetime τ_{nr}, or low mobility, led to differences between EQE and PLE efficiencies, both in shape and magnitude. In this context, extension of the study to thin-film, polycrystalline solar cells may highlight such differences between the two spectra, and provide a more general validation of the usefulness of the technique.

REFERENCES

[1] R. Ahrenkiel, "Measurement of minority-carrier lifetime by time-resolved photoluminescence," *Solid-state Electron.*, vol. 35, no. 3, pp. 239–250, 1992.

[2] J. Dishman, "Characterization of dominant recombination centers in semiconductors from the temperature dependence of luminescence excitation spectra: GaP (Zn, O)," *Phys. Rev. B*, vol. 5, no. 6, pp. 2258–2267, 1972.

[3] B. Monemar, "Fundamental energy gap of GaN from photoluminescence excitation spectra," *Phys. Rev. B*, vol. 10, no. 2, pp. 676–681, 1974.

[4] T. Sawada, K. Numata, S. Tohdoh, T. Saitoh, and H. Hasegawa, "*In situ* characterization of compound semiconductor surfaces by novel photoluminescence surface state spectroscopy," *Japan. J. Appl. Phys.*, vol. 32, pp. 511–511, 1993.

[5] G. D. Pettit, J. M. Woodall, and H. J. Hovel, "Photoluminescent characterization of GaAs solar cells," *Appl. Phys. Lett.*, vol. 35, no. 4, pp. 335–337, 1979.

[6] J. M. Woodall, G. D. Pettit, T. Chappell, and H. J. Hovel, "Photoluminescent properties of Gaas–GaAlAs, GaAs–oxide, and GaAs–ZnS heterojunctions," *J. Vacuum Sci. Technol.*, vol. 16, no. 5, pp. 1389–1393, 1979.

[7] U. Rau, "Reciprocity relation between photovoltaic quantum efficiency and electroluminescent emission of solar cells," *Phys. Rev. B*, vol. 76, pp. 085303-1–085303-8, Aug. 2007.

[8] U. Rau, "Superposition and reciprocity in the electroluminescence and photoluminescence of solar cells," *IEEE J. Photovolt.*, vol. 2, no. 2, pp. 169–172, Apr. 2012.

[9] M. Green, "Radiative efficiency of state-of-the-art photovoltaic cells," *Progr. Photovolt.: Res. Appl.*, vol. 20, no. 4, pp. 472–476, 2011.

[10] J. L. Gray and M. McLennan. (2007, May). Adept solar cell simulator. [Online]. Available: https://nanohub.org/resources/2658

[11] X. Wang, M. Khan, J. Gray, M. Alam, and M. Lundstrom, "Design of GaAs solar cells operating close to the Shockley-Queisser limit," *IEEE J. Photovolt.*, vol. 3, no. 2, pp. 737–744, Apr. 2013.

[12] S. Adachi, "Optical dispersion relations for GaP, GaAs, GaSb, InP, InAs, InSb, AlGaAs, and InGaAsP," *J. Appl. Phys.*, vol. 66, pp. 6030-1–6030-11, 1989.

[13] R. Haitz and J. Y. Tsao, "Solid-state lighting: The case 10 years after and future prospects," *Phys. Status Solidi A*, vol. 208, no. 1, pp. 17–29, 2011.

[14] J. S. Bhosale, "High signal-to-noise Fourier transform spectroscopy with light emitting diode sources," *Rev. Sci. Instrum.*, vol. 82, no. 9, pp. 093103-1–093103-4, 2011.

[15] H. Hasegawa, H. Ishii, T. Sawada, T. Saitoh, S. Konishi, Y. Liu, and H. Ohno, "Control of fermi level pinning and recombination processes at gaas surfaces by chemical and photochemical treatments," *J. Vacuum Sci. Technol. B: Microelectron. Nanometer Struct.*, vol. 6, no. 4, pp. 1184–1192, 1988.

[16] O. D. Miller, E. Yablonovitch, and S. R. Kurtz, "Strong internal and external luminescence as solar cells approach the Shockley–Queisser limit," *IEEE J. Photovolt.*, vol. 2, no. 3, pp. 303–311, Jul. 2012.

Authors' photographs and biographies not available at the time of publication.